

S factor of $^{13}\text{C}(\alpha,n)^{16}\text{O}$ at low energies in cluster effective field theory

Shung-Ichi Ando¹,

*Department of Display and Semiconductor Engineering and Research
Center for Nano-Bio Science, Sunmoon University, Asan, Chungnam
31460, Republic of Korea*

*Department of Physics Education, Daegu University, Gyeongsan 38453,
Republic of Korea*

The $^{13}\text{C}(\alpha,n)^{16}\text{O}$ reaction at low energies is studied by constructing an effective field theory. We choose a separation scale at $E = 1$ MeV, where E is the initial α - ^{13}C energy in center-of-mass frame, just below the sharp resonant $5/2^+$ state of ^{17}O , and include two open channels, α - ^{13}C and n - ^{16}O , and resonant $1/2^+$, $5/2^-$, $3/2^+$ states of ^{17}O in the study. Parameters of the theory are fitted to experimental data, S factor of $^{13}\text{C}(\alpha,n)^{16}\text{O}$ at the energies below $E = 1$ MeV, including the data sets recently reported by the LUNA and JUNA collaborations, and the S factor of $^{13}\text{C}(\alpha,n)^{16}\text{O}$ is extrapolated to the Gamow peak energy $E_G = 0.19$ MeV in the low mass AGB stars. We discuss an uncertainty in the estimate of the S factor and confirm that the main part of the uncertainty emerges from the parameter fit of the near-breakup threshold $1/2^+$ state of ^{17}O .

¹<mailto:sando@sunmoon.ac.kr>

1. Introduction

The $^{13}\text{C}(\alpha, n)^{16}\text{O}$ reaction provides a main neutron source in s process in low mass asymptotic giant branch (AGB) stars with the mass $1.5 \leq M/M_{\odot} \leq 3$ [1]. A ^{13}C pocket, where ^{13}C is produced through $^{12}\text{C}(p, \gamma)^{13}\text{N}(\beta^+ \nu)^{13}\text{C}$, is formed in a thin (He-rich and C-rich) He-intershell between a compact C-O core and an expanded H-rich envelope at the epoch of the so-called third dredge up. The $^{13}\text{C}(\alpha, n)^{16}\text{O}$ reaction takes place during the interpulse phase of the AGB stars, $\sim 10^4$ yr, when the temperature rises up to $\sim 90 \times 10^6$ K. It leads to a maximum neutron density about 10^7 cm^{-3} . By neutron capture reactions (and following β decay reactions) heavier elements, $Z > 30$, are synthesized through the line of stability. About half of the heavy elements in the universe have been created in the s process in the low mass AGB stars [2].

Recently, precise measurements of the $^{13}\text{C}(\alpha, n)^{16}\text{O}$ reaction were reported from the LUNA collaboration [3] and the JUNA collaboration [4], and the energy ranges of the measurements are $E = 230$ to 300 keV and 240 to 1800 keV, respectively. They are close to the Gamow peak energy, $E_G = 190 \pm 40$ keV, for the α - ^{13}C system at $\sim 90 \times 10^6$ K. It may be straightforward to extrapolate the cross section, equivalently the astrophysical S factor, of the $^{13}\text{C}(\alpha, n)^{16}\text{O}$ reaction to E_G with the new data, but an uncertainty in the estimate of the S factor emerges from the low-energy side of the experimental data, due to a broad resonant $1/2^+$ state of ^{17}O appearing around the breakup energy of the α - ^{13}C channel [5]. In this work, we construct an effective field theory (EFT) for the study of the $^{13}\text{C}(\alpha, n)^{16}\text{O}$ reaction, extrapolate the S factor to E_G , and confirm the uncertainty from the near-threshold state.

An EFT for the study of a reaction in question is constructed by introducing a separation scale between relevant degrees of freedom at low energies and irrelevant degrees of freedom at high energies [6, 7]. An effective Lagrangian is constructed by requiring symmetries and is expanded in terms of the number of derivatives on the fields. The theory provides us with a perturbative expansion scheme in powers of \mathcal{Q}/Λ_H where \mathcal{Q} is a typical momentum scale and Λ_H is a large momentum scale, and the reaction amplitudes are calculated order by order. The infinities from loop calculations, where the loops preserve the unitary condition of the amplitudes, are subtracted by the coefficients of the effective Lagrangian; the contributions from the irrelevant degrees of freedom at high energies are embedded in the coefficients, while the coefficients are practically fitted to experimental data. The perturbative expansion scheme in an EFT would be useful to estimate a systematic uncertainty due to the truncation of perturbative series. For the last decade, we applied the methodology of EFT to the study of nuclear reactions for nuclear astrophysics. We constructed an EFT for α - ^{12}C system and studied elastic α - ^{12}C scattering [8, 9, 10, 11], β delayed α emission from ^{16}N [12], and $E1$ and $E2$ transitions of $^{12}\text{C}(\alpha, \gamma)^{16}\text{O}$ reaction [13, 14, 15].

In this work, we construct an EFT for the study of $^{13}\text{C}(\alpha, n)^{16}\text{O}$ reaction at low energies and extrapolate the S factor of the reaction to E_G . As we will discuss in the next section, we introduce three resonant $1/2^+$, $5/2^-$, $3/2^+$ states of ^{17}O as relevant degrees of freedom in the present study, and we employ composite fields for them. At the energy region close to the resonant poles, one needs to treat interactions non-perturbatively [16]. By

employing composite fields, one can expand the terms in the unitary limits: those terms are matched to the effective range parameters [17, 18, 19]. We also introduce two open channels, α - ^{13}C and n - ^{16}O . To construct projection operators of the two open channels to the resonant fields for the $3/2^+$ and $5/2^-$ states, we employ the 2×4 matrices for the $3/2^+$ state reported by Fernando, Higa, and Rupak [20]. For the projection operators to connect the two open channels to the $5/2^-$ state, we construct the 2×6 matrices. We write down the effective Lagrangian, extract the vertices and propagators from the Lagrangian, and calculate the vertices and self-energies, including the non-perturbative Coulomb interaction. Then, we obtain an expression for the reaction amplitudes of $^{13}\text{C}(\alpha, n)^{16}\text{O}$ for the three resonant states of ^{17}O in EFT. The parameters in the theory are fitted to the available experimental data of the S factor at $0.23 \leq E \leq 1$ MeV, and the S factor is extrapolated to $E_G = 0.19$ MeV. We then discuss the uncertainties of the estimate of the S factor in this work.

The present work is organized as follows. In Section 2, we discuss the composition of an EFT for the $^{13}\text{C}(\alpha, n)^{16}\text{O}$ reaction at low energies, and in Section 3, the effective Lagrangian for the present work is presented. In Section 4, the expressions of S factors and reaction amplitudes are displayed. In Section 5, the numerical results of this work are reported, and in Section 6, the results and discussions of this work are presented. In the appendices, we discuss the calculation of the components of the amplitudes in detail. In Appendix A, the projection operators for the $1/2^+$, $5/2^-$, $3/2^+$ states are discussed, and in Appendix B, the angular momentum projection operators for $l = 1, 2, 3$ between the two clusters of the open channels are displayed. In Appendix C, the expressions of the components of the reaction amplitudes; bare propagators, vertex functions, self-energies, and dressed propagators, are displayed and discussed.

2. Composing an EFT of $^{13}\text{C}(\alpha, n)^{16}\text{O}$ at low energies

In this section, we compose an effective theory for the study of $^{13}\text{C}(\alpha, n)^{16}\text{O}$ at low energies. We study the reaction



where the energy difference of the two channels, namely the Q value, is $Q = 2.2156$ MeV.² We chose a typical energy of the reaction for this study as the Gamow peak energy at $T \simeq 90 \times 10^6$ K in the low mass AGB stars. It would be $E = 190 \pm 40$ keV, where E is the energy of the initial α - ^{13}C system in the center-of-mass frame. The typical momentum scales would be $\mathcal{Q} = \sqrt{2\mu_{\alpha\text{C}}E_G} = 33$ MeV where $\mu_{\alpha\text{C}}$ is the reduced mass of α - ^{13}C system, and we have fixed the Gamow peak energy at $E_G = 0.19$ MeV. Because the typical length scale, $\hbar c/\mathcal{Q} = 6.0$ fm, is large compared to the sizes of the nuclei, we introduce the neutron and nuclei as point-like particles.

The spin, parity, and isospin states of the ground states of the nuclei and neutron are

$$^{13}\text{C}(1/2^-; 1/2), \alpha(0^+; 0), ^{16}\text{O}(0^+; 0), n(1/2^+; 1/2), \quad (2)$$

²When we set the zero energy at the ground state of ^{17}O , the threshold energies of n - ^{16}O and α - ^{13}C channels are 4.14 MeV and 6.359 MeV, respectively.

J^π	E_x (MeV)	Γ (keV)	E (MeV)	α - ^{13}C	n - ^{16}O
$1/2^+$	6.356(8)	124(12)	-0.003(8)	$l = 1$	$l = 0$
$5/2^-$	7.16586(17)	1.38(5)	0.80686(17)	$l = 2$	$l = 3$
$3/2^+$	7.202(10)	280(30)	0.843(10)	$l = 1$	$l = 2$

Table 1: Energies and widths of the resonant states of ^{17}O near the α - ^{13}C breakup threshold energy [21]. E is the energy of the α - ^{13}C system where $E = E_x - S_\alpha$; S_α is the α separation energy from ^{17}O is $S_\alpha = 6.359$ MeV. In the fourth and fifth columns, the relative angular momenta between two clusters for α - ^{13}C and n - ^{16}O channels are presented.

and, in this work, we assume that the reaction occurs through the resonance states of ^{17}O , which are effective around the energy of the initial α - ^{13}C state. There is no bound state of ^5He , and the breakup energy of ^{13}C in n - ^{12}C channel is 4.94635 MeV and the energy of the first excited state of ^{13}C is 3.089 MeV. They are significantly larger than the energy, $E = 1$ MeV, at which we truncate the data set for parameter fit in this work. Thus, ^5He - ^{12}C and n - α - ^{12}C channels are regarded as irrelevant degrees of freedom at high energies. We may employ the two channels,

$$\alpha + ^{13}\text{C}, \quad n + ^{16}\text{O}, \quad (3)$$

are relevant degrees of freedom at low energies and describe the reaction in terms of the resonant states of ^{17}O .

It is known that there are three resonant states of ^{17}O close to the α - ^{13}C breakup threshold energy [21], at $E_x = 6.356(8)$ MeV with $\Gamma = 124(12)$ keV ($J^\pi = 1/2^+$), $E_x = 7.16586(17)$ MeV with $\Gamma = 1.38(5)$ keV ($J^\pi = 5/2^-$), and $E_x = 7.202(10)$ MeV with $\Gamma = 280(30)$ keV ($J^\pi = 3/2^+$), while we choose the sharp resonant $5/2^+$ state at $E_x = 7.3792(10)$ MeV, $\Gamma = 0.64(23)$ keV as an irrelevant state at high energy, and we truncate the data set for the parameter fit, just below the $5/2^+$ state, at $E = 1$ MeV. We introduce the three resonant $1/2^+$, $5/2^-$, $3/2^+$ states of ^{17}O in the theory. In Table 1, we summarize the states and also listed the relative angular momenta between two clusters of α - ^{13}C and n - ^{16}O channels to describe the resonant states of ^{17}O .

We have chosen the typical momentum scale as $Q = 33$ MeV for the reaction in the low mass AGB stars above. Some large energy scales in the present study can be listed up as follows: the first resonant $1/2^+$ state of ^{13}C , $E = 3.089$ MeV, the breakup threshold energy of the n - α - ^{12}C channel, $E = 4.95$ MeV, and a broad resonant $3/2^-$ state of ^{17}O at $E_x = 7.542(20)$ MeV and $\Gamma = 500(50)$ keV, which appears at $E = 1.183$ MeV. So we may choose a high energy scale as $E_H = 1.2$ MeV, and the large momentum scale is $\Lambda_H = \sqrt{2\mu_{\alpha C} E_H} = 82$ MeV. Thus, we have the parameter of the perturbative expansion as $Q/\Lambda_H = 0.4$. We note that because momentum is a vector, and, in many cases, the corrections appear as a power of a scalar quantity, $(Q/\Lambda_H)^2 = 0.16$.³

³In this study, we have very large quantities compared to the large scale, $\Lambda_H = 82$ MeV, such as the reduced masses, $\mu_{\alpha C} = 2850$ MeV and $\mu_{nO} = 884$ MeV, and the inverse of the Bohr radius of the α - ^{13}C

3. Effective Lagrangian

In this section, we construct the effective Lagrangian for the study of $^{13}\text{C}(\alpha, n)^{16}\text{O}$ at low energies. As discussed in the previous section, we have introduced the α - ^{13}C and n - ^{16}O channels and the resonant $1/2^+$, $5/2^-$, $3/2^+$ states of ^{16}O in this study. The effective Lagrangian for the present study is presented as

$$\mathcal{L} = \mathcal{L}_0 + \mathcal{L}_R + \mathcal{L}_{int}, \quad (4)$$

where \mathcal{L}_0 is the Lagrangian for α , ^{13}C , n , and ^{16}O in the initial and final states, \mathcal{L}_R is that for the resonant states of ^{17}O , and \mathcal{L}_{int} is that for the interactions of the fields.

The Lagrangian \mathcal{L}_0 is standard and one has

$$\begin{aligned} \mathcal{L}_0 = & \phi_\alpha^* \left(i\partial_0 + \frac{1}{2m_\alpha} \nabla^2 \right) \phi_\alpha + \psi_{^{13}\text{C}}^\dagger \left(i\partial_0 + \frac{1}{2m_{^{13}\text{C}}} \nabla^2 \right) \psi_{^{13}\text{C}} \\ & + \psi_n^\dagger \left(i\partial_0 + \frac{1}{2m_n} \nabla^2 \right) \psi_n + \phi_O^* \left(i\partial_0 + \frac{1}{2m_O} \nabla^2 \right) \phi_O, \end{aligned} \quad (5)$$

where ϕ_α and ϕ_O are non-relativistic scalar fields for α and ^{16}O and ψ_n and $\psi_{^{13}\text{C}}$ are non-relativistic spin-1/2 fields for n and ^{13}C . The expressions of the inverse propagators of those fields are presented in Appendix C.

The Lagrangian \mathcal{L}_R for the resonant states of ^{17}O as non-relativistic fields is given as

$$\begin{aligned} \mathcal{L}_R = & \sum_{n=0}^N C_{1p}^{(n)} d_{1p}^\dagger \left(i\partial_0 + \frac{1}{2m_{1p}} \nabla^2 \right)^n d_{1p} + \sum_{n=0}^N C_{5m}^{(n)} d_{5m}^\dagger \left(i\partial_0 + \frac{1}{2m_{5m}} \nabla^2 \right)^n d_{5m} \\ & + \sum_{n=0}^N C_{3p}^{(n)} d_{3p}^\dagger \left(i\partial_0 + \frac{1}{2m_{3p}} \nabla^2 \right)^n d_{3p}, \end{aligned} \quad (6)$$

where d_{1p} , d_{5m} , d_{3p} , are the fields for the resonant $1/2^+$, $5/2^-$, $3/2^+$ states of ^{17}O , and $C_{1p}^{(n)}$, $C_{5m,j}^{(n)}$, $C_{3p}^{(n)}$ are the coupling constants to renormalize the infinities from self-energy terms, and the values of the constants are fixed by using the experimental data. d_{1p} is the two-component spin-1/2 spinor, d_{5m} is the six-component spin-5/2 spinor, and d_{3p} is the four-component spin-3/2 spinor. m_{1p} , m_{5m} , m_{3p} are the masses corresponding to the resonant states of ^{17}O . We note that, when one chooses the center-of-mass frame, the total three momenta of the fields vanish; one does not need to know the values of the masses of the resonant states. In the present work, we choose the number of the expansion terms, $N = 1$, for the $1/2^+$ and $5/2^-$ states and $N = 3$ for the $3/2^+$ state. The expressions of the inverse of the bare propagators are presented in Appendix C.

The Lagrangian \mathcal{L}_{int} to describe the interactions between the resonant states and the two cluster states is given as

$$\mathcal{L}_{int} = -y_{1p} \left[d_{1p}^\dagger \left(P_{1/2^+,i}^{(l=1)} \psi_{^{13}\text{C}} O_i^{(l=1)} \phi_\alpha \right) + \left(P_{1/2^+,i}^{(l=1)} \psi_{^{13}\text{C}} O_i^{(l=1)} \phi_\alpha \right)^\dagger d_{1p} \right]$$

system, $\kappa = Z_\alpha Z_{^{13}\text{C}} \alpha_E \mu_{\alpha\text{C}} = 249.6 \text{ MeV}$ where Z_α and $Z_{^{13}\text{C}}$ are the numbers of protons in the nuclei and α_E is the fine structure constant.

$$\begin{aligned}
& -y'_{1p} \left[d_{1p}^\dagger \left(P_{1/2^+}^{(l=0)} \psi_n O^{(l=0)} \phi_O \right) + \left(P_{1/2^+}^{(l=0)} \psi_n O^{(l=0)} \phi_O \right)^\dagger d_{1p} \right] \\
& -y'_{5m} \left[d_{5m}^\dagger \left(P_{5/2^-,ij}^{(l=2)} \psi_{13C} O_{ij}^{(l=2)} \phi_\alpha \right) + \left(P_{5/2^-,ij}^{(l=2)} \psi_{13C} O_{ij}^{(l=2)} \phi_\alpha \right)^\dagger d_{5m} \right] \\
& -y'_{5m} \left[d_{5m}^\dagger \left(P_{5/2^-,ijk}^{(l=3)} \psi_n O_{ijk}^{(l=3)} \phi_O \right) + \left(P_{5/2^-,ijk}^{(l=3)} \psi_n O_{ijk}^{(l=3)} \phi_O \right)^\dagger d_{5m} \right] \\
& -y'_{3p} \left[d_{3p}^\dagger \left(P_{3/2^+,i}^{(l=1)} \psi_{13C} O_i^{(l=1)} \phi_\alpha \right) + \left(P_{3/2^+,i}^{(l=1)} \psi_{13C} O_i^{(l=1)} \phi_\alpha \right)^\dagger d_{3p} \right] \\
& -y'_{3p} \left[d_{3p}^\dagger \left(P_{3/2^+,ij}^{(l=2)} \psi_n O_{ij}^{(l=2)} \phi_O \right) + \left(P_{3/2^+,ij}^{(l=2)} \psi_n O_{ij}^{(l=2)} \phi_O \right)^\dagger d_{3p} \right], \tag{7}
\end{aligned}$$

where $P_{1/2^+}^{(l=0)}$, $P_{1/2^+}^{(l=1)}$, $P_{5/2^-}^{(l=2)}$, $P_{5/2^-}^{(l=3)}$, $P_{3/2^+}^{(l=1)}$, $P_{3/2^+}^{(l=2)}$ are the projection operators of the two cluster states to $J^\pi = 1/2^+$, $J^\pi = 5/2^-$, $J^\pi = 3/2^+$ states with the relative angular momenta $l = 0, 1, 2, 3$. $O^{(l=0)}$, $O_i^{(l=1)}$, $O_{ij}^{(l=2)}$, $O_{ijk}^{(l=3)}$, are the projection operators of the two cluster channels for $l = 0, 1, 2, 3$ states, respectively. The expressions of the projection operators of the relative angular momenta, $O^{(l=0)}$, $O_i^{(l=1)}$, $O_{ij}^{(l=2)}$, $O_{ijk}^{(l=3)}$, are presented in Appendix B.

For the α - ^{13}C channel, we have the projection operators, $P_{1/2^+,i}^{(l=1)}$, $P_{5/2^-,ij}^{(l=2)}$, $P_{3/2^+,i}^{(l=1)}$, as

$$P_{1/2^+,i}^{(l=1)} = -\frac{1}{\sqrt{3}} \sigma_i^T, \quad P_{5/2^-,ij}^{(l=2)} = \frac{1}{\sqrt{5}} R_i^T L_j^T, \quad P_{3/2^+,i}^{(l=1)} = S_i^T, \tag{8}$$

where σ_i are the Pauli matrices and S_i are spin-1/2 to spin-3/2 projection matrices [20]. In addition, $(M_{ji} =) L_j R_i$ are spin-1/2 to spin-5/2 projection matrices. For the n - ^{16}O channel, we have the projection operators, $P_{1/2^+}^{(l=0)}$, $P_{5/2^-,ijk}^{(l=2)}$, $P_{3/2^+,ij}^{(l=2)}$, as

$$P_{1/2^+}^{(l=0)} = 1, \quad P_{5/2^-,i}^{(l=3)} = -\frac{1}{\sqrt{15}} R_i^T L_j^T \sigma_k^T, \quad P_{3/2^+,ij}^{(l=2)} = -\sqrt{\frac{2}{5}} S_i^T \sigma_j^T. \tag{9}$$

In Appendix A, the expressions of the matrices, S_i , L_j , R_k , are presented and the projection operators are discussed in detail.

4. S factors and reaction amplitudes

The S factor of the $^{13}\text{C}(\alpha, n)^{16}\text{O}$ reaction in the center-of-mass frame is defined by

$$S = \sigma(E) E \exp(2\pi\eta), \tag{10}$$

where $\sigma(E)$ is the total cross section and η is the Sommerfeld parameter. The total cross section is presented as

$$\sigma(E) = \int d\Omega_{\hat{p}'} \frac{d\sigma(E)}{d\Omega_{\hat{p}'}} = \frac{\mu' \mu p'}{8\pi^2 p} \int d\Omega_{\hat{p}'} \sum_{spin} |A|^2, \tag{11}$$

where $\mu' = \mu_{nO}$ and $\mu = \mu_{\alpha^{13}\text{C}}$, and μ_{nO} and $\mu_{\alpha^{13}\text{C}}$ are the reduced masses of n - ^{16}O and α - ^{13}C , respectively. p' and p are the magnitudes of the relative momenta of the final n - ^{16}O

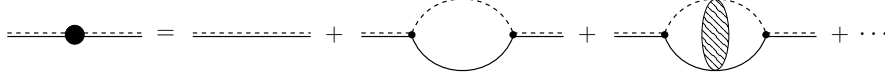


Figure 1: Diagrams for dressed ^{17}O propagators. A thick and thin double-dashed line with and without a filled circle represent a dressed and bare ^{17}O propagators, respectively. A loop diagram with (without) a shaded ellipse represents the n - ^{16}O (α - ^{13}C) self-energy term. A shaded ellipse represents the Coulomb Green's function.

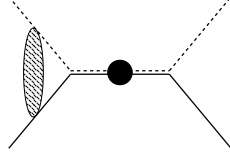


Figure 2: Feynman diagram of the amplitudes of $^{13}\text{C}(\alpha, n)^{16}\text{O}$ reaction. A line (dashed line) in the initial state represents a propagator of ^{13}C (α), and a line (dashed line) in the final state represents a propagator of n (^{16}O). A shaded ellipse in the initial state represents the Coulomb wavefunction. See the caption in Fig. 1 as well.

and initial α - ^{13}C states, respectively, $p' = \sqrt{2\mu'(E + Q)}$ and $p = \sqrt{2\mu E}$, where Q is the Q value of the reaction. A is the reaction amplitude.

We decompose the S factor as

$$S = S_{1p} + S_{5m} + S_{3p}, \quad (12)$$

where S_{1p} , S_{5m} , S_{3p} are the S factors obtained from the reaction amplitudes for the resonant $1/2^+$, $5/2^-$, $3/2^+$ states of ^{17}O , respectively. The reaction amplitudes, A_{1p} , A_{5m} , A_{3p} , for S_{1p} , S_{5m} , S_{3p} , respectively, are calculated from Feynman diagrams in Figs. 1 and 2. In the following subsections, we construct the reaction amplitudes and S factors for the resonant $1/2^+$, $5/2^-$, $3/2^+$ states of ^{17}O , while we display and discuss in detail the components of the amplitudes, vertex functions, initial Coulomb wavefunctions, self-energies, and dressed propagators of the resonant states of ^{17}O in Appendix C.

4.1 Reaction amplitude and S factor for the $1/2^+$ resonant state of ^{17}O

We have the reaction amplitude for the $1/2^+$ resonant state of ^{17}O as

$$\begin{aligned} A_{1p} &= -\Gamma_{dnO}^{(1p)} D_{1p}(p) \Psi_{d\alpha C}^{(1p)}(p) \\ &= -\frac{2\pi}{\sqrt{3}\mu} \frac{e^{i\sigma_1} \sqrt{p^2 + \kappa^2} C_\eta \chi_n^\dagger \vec{\sigma}^T \cdot \hat{p} \chi_C}{\sum_{n=0}^N \frac{2\pi}{y^y} C_{1p}^{(n)} E^n + \frac{1}{3\mu} \left(\frac{y}{y'} 2\kappa H_1(p) \right) + i\mu' \frac{y'}{y} p'}, \end{aligned} \quad (13)$$

where $\Psi_{d\alpha C}^{(1p)}(p)$ is the vertex function of the initial α - ^{13}C state for $l = 1$ including the initial Coulomb wavefunction to d_{1p} , $D_{1p}(p)$ is the dressed propagator of the resonant $1/2^+$ state of ^{17}O , and $\Gamma_{dnO}^{(1p)}$ is the vertex function of d_{1p} to the final n - ^{16}O state for $l = 0$.

Those three components of the amplitude are presented in Appendix C. In addition, σ_1 is the Coulomb phase shift for $l = 1$, and the function $H_1(p)$ is obtained as⁴

$$H_1(p) = W_1(p)H(\eta) = (p^2 + \kappa^2)H(\eta), \quad (14)$$

with

$$H(\eta) = \psi(i\eta) + \frac{1}{2i\eta} - \log(i\eta), \quad (15)$$

where η is the Sommerfeld parameter, $\eta = \kappa/p$, κ is the inverse of the Bohr radius of the α -¹³C system, $\kappa = Z_\alpha Z_{13C} \mu \alpha_E$; Z_α and Z_{13C} are the numbers of protons in the nuclei and α_E is the fine structure constant, $\alpha_E = 1/137.036$. $\psi(z)$ is the digamma function.

Using a relation

$$2\kappa \text{Im}H_1(p) = p(p^2 + \kappa^2)C_\eta^2, \quad (16)$$

where

$$C_\eta^2 = \frac{2\pi\eta}{\exp(2\pi\eta) - 1}, \quad (17)$$

we define the α and neutron vertices for the ¹³C(α, n)¹⁶O reaction for the resonant $1/2^+$ state of ¹⁷O as

$$\Gamma_{1p}^\alpha(E) = 2Z_{1p}p(p^2 + \kappa^2)C_\eta^2, \quad (18)$$

$$\Gamma_{1p}^n(E) = 6Z_{1p}\mu'\mu\frac{y'^2}{y^2}p' = \Gamma_{R(1p)}^n\sqrt{\frac{E+Q}{-B+Q}}, \quad (19)$$

where Z_{1p} is a wavefunction normalization factor and $\Gamma_{R(1p)}^n$ is the neutron width of the $1/2^+$ state at $E = -B$. Z_{1p} is obtained when the function, $2\kappa H_1(p)$, is normalized in the denominator of the amplitude as

$$\frac{6\pi\mu}{y^2} \sum C_{1p}^{(n)} E^n + 2\kappa \text{Re}H_1(p) = Z_{1p}^{-1} (E + B + \dots), \quad (20)$$

where the inverse of the propagator should vanish at $E = -B$, and we neglect the higher order terms, denoted by the dots, in the denominator of the amplitude for the $1/2^-$ state. The wavefunction normalization factor, Z_{1p} , is related to the asymptotic normalization coefficient (ANC) of the $1/2^+$ state of ¹⁷O, as a bound state of the α -¹³C system, by using a formula [22],

$$|C_b|_{1p} = \gamma_{1p}\Gamma(2 + \kappa/\gamma_{1p})\sqrt{2\mu Z_{1p}}, \quad (21)$$

⁴ $H_l(p)$ functions are defined as [10]

$$H_l(p) = W_l(p)H(\eta), \quad W_l(p) = \left(\frac{\kappa^2}{l^2} + p^2\right)W_{l-1}(p), \quad W_0(p) = 1.$$

where γ_{1p} is the binding momentum of the $1/2^+$ state of ^{17}O , $\gamma_{1p} = \sqrt{2\mu B}$, and $\Gamma(z)$ is the gamma function.

Thus, we have the reaction amplitude of the $1/2^+$ state of ^{17}O as

$$A_{1p} = -\frac{\pi}{\sqrt{\mu'\mu p'p}} \frac{e^{i\sigma_1} \sqrt{\Gamma_{1p}^\alpha(E)\Gamma_{1p}^n(E)}}{E + B + i\frac{1}{2}(\Gamma_{1p}^\alpha(E) + \Gamma_{1p}^n(E))} \chi_n^\dagger \vec{\sigma}^T \cdot \hat{p} \chi_C, \quad (22)$$

and the S factor of the $1/2^+$ resonant state of ^{17}O is obtained as

$$S_{1p} = \frac{\pi}{2\mu} \frac{\Gamma_{1p}^\alpha(E)\Gamma_{1p}^n(E)e^{2\pi\eta}}{(E + B)^2 + \frac{1}{4}(\Gamma_{1p}^\alpha(E) + \Gamma_{1p}^n(E))^2}. \quad (23)$$

The S_{1p} factor has three parameters, B , Z_{1p} , and $\Gamma_{R(1p)}^n$. In this work, we fix $B = 3$ keV and two parameters, Z_{1p} and $\Gamma_{R(1p)}^n$, are fitted to the experimental data.

4.2 Reaction amplitude and S factor for $5/2^-$ state of ^{17}O

The reaction amplitude of $^{13}\text{C}(\alpha, n)^{16}\text{O}$ for the resonant $5/2^-$ state of ^{17}O is

$$\begin{aligned} A_{5m} &= -\Gamma_{dnO}^{(5m)}(p') D_{5m}(p) \Psi_{d\alpha C}^{(5m)}(p) \\ &= -\frac{1}{10\sqrt{3}} \frac{y'y}{\mu'^3\mu^2} \frac{\chi_n^\dagger \vec{\sigma}^* \cdot \vec{p}' \vec{L}^* \cdot \vec{p}' \vec{R}^* \cdot \vec{p}' \vec{R}^T \cdot \vec{p}' \vec{L}^T \cdot \vec{p} \chi_C e^{i\sigma_2} \sqrt{(1+\eta^2)(4+\eta^2)} C_\eta}{\sum_{n=0}^N C_{5m}^{(n)} E^n + \frac{2y^2}{15\mu^4} \left(\frac{\mu}{2\pi} 2\kappa H_2(p) \right) + i \frac{2y'^2}{45\mu'^6} \frac{\mu'}{2\pi} p'^7} \end{aligned} \quad (24)$$

where $\Psi_{d\alpha C}^{(5m)}(p)$ is the vertex function of the α - ^{13}C state for $l = 2$ including the initial Coulomb wavefunction to d_{5m} , $D_{5m}(p)$ is the dressed propagator of the $5/2^-$ state of ^{17}O , and $\Gamma_{dnO}^{(5m)}(p')$ is the vertex function of $d_{(5m)}$ to the n - ^{16}O state for $l = 3$. Those three components of the amplitude are presented in Appendix C. σ_2 is the Coulomb phase shift for $l = 2$, and the function $H_2(p)$ is given as

$$H_2(p) = W_2(p)H(\eta) = \frac{1}{4}p^4(1+\eta^2)(4+\eta^2)H(\eta). \quad (25)$$

Using a relation,

$$2\kappa \text{Im}H_2(p) = \frac{1}{4}p(p^2 + \kappa^2)(4p^2 + \kappa^2)C_\eta^2, \quad (26)$$

and a similar relation to Eq. (20) to define Z_{5m} , where Z_{5m} is the wavefunction normalization factor, we define the α and neutron vertices as

$$\Gamma_{5m}^\alpha(E) = 2Z_{5m}pW_2(p)C_\eta^2 = \Gamma_{R(5m)}^\alpha \frac{pW_2(p)C_\eta^2}{p_rW_2(p_r)C_{\eta_r}^2}, \quad (27)$$

$$\Gamma_{5m}^n(E) = Z_{5m} \frac{2\mu^3 y'^2}{3\mu'^5 y^2} p'^7 = \Gamma_{R(5m)}^n \left(\frac{E + Q}{E_{R(5m)} + Q} \right)^{7/2}, \quad (28)$$

where p_r and $\eta_r = \kappa/p_r$ are the momentum and Sommerfeld factor at $E = E_{R(5m)}$, $p_r = \sqrt{2\mu E_{R(5m)}}$; $E_{R(5m)}$ is the resonant energy of the $5/2^-$ state of ^{17}O . $\Gamma_{R(5m)}^\alpha$ and $\Gamma_{R(5m)}^n$ are the α and neutron widths of the $5/2^-$ state at $E = E_{R(5m)}$. We note that because $\Gamma_{R(5m)}^\alpha$ and $\Gamma_{R(5m)}^n$ are fitted to the experimental data, the factor Z_{5m} can be an arbitrary constant. Thus, we have the reaction amplitude of the $^{13}\text{C}(\alpha, n)^{16}\text{O}$ reaction of the resonant $5/2^-$ state of ^{17}O as

$$A_{5m} = -\frac{3\pi}{2\sqrt{\mu'\mu p'p}} \frac{\chi_n^\dagger \vec{\sigma}^* \cdot \hat{p}' \vec{L}^* \cdot \hat{p}' \vec{R}^* \cdot \hat{p}' \vec{R}^T \cdot \hat{p}' \vec{L}^T \cdot \hat{p} \chi_C e^{i\sigma_2} \sqrt{\Gamma_{5m}^n(E) \Gamma_{5m}^\alpha(E)}}{E - E_{R(5m)} + i\frac{1}{2}(\Gamma_{5m}^n(E) + \Gamma_{5m}^\alpha(E))}. \quad (29)$$

To calculate the squared amplitude and angle integral in the phase space, we have

$$\int \frac{d\Omega_{\hat{p}'}}{4\pi} \text{Tr} \left(\vec{R}^\dagger \cdot \hat{p}' \vec{L}^\dagger \cdot \hat{p}' \vec{\sigma}^\dagger \cdot \hat{p}' \vec{\sigma} \cdot \hat{p}' \vec{L} \cdot \hat{p}' \vec{R} \cdot \hat{p}' \vec{R}^\dagger \cdot \hat{p}' \vec{L}^\dagger \cdot \hat{p}' \vec{L} \cdot \hat{p}' \vec{R} \cdot \hat{p} \right)^* = \frac{8}{3}, \quad (30)$$

where we have chosen $\hat{p} = (0, 0, 1)$. Thus, we have the S factor of the $5/2^-$ state of ^{17}O as

$$S_{5m} = \frac{3\pi}{2\mu} \frac{\Gamma_{5m}^n(E) \Gamma_{5m}^\alpha(E) e^{2\pi\eta}}{(E - E_{R(5m)})^2 + \frac{1}{4}(\Gamma_{5m}^n(E) + \Gamma_{5m}^\alpha(E))^2}. \quad (31)$$

The S_{5m} factor has three parameters, $E_{R(5m)}$, $\Gamma_{R(5m)}^n$, $\Gamma_{R(5m)}^\alpha$. Those parameters are fitted to the experimental data.

4.3 Reaction amplitude and S factor for $3/2^+$ state of ^{17}O

The reaction amplitude of $^{13}\text{C}(\alpha, n)^{16}\text{O}$ for the resonant $3/2^+$ state of ^{17}O is

$$\begin{aligned} A_{3p} &= -\Gamma_{dnO}^{(3p)}(p') D_{3p}(p) \Psi_{d\alpha C}^{(3p)}(p) \\ &= -\sqrt{\frac{2}{5}} \frac{y'y}{\mu'^2 \mu} \frac{\chi_n^\dagger \vec{\sigma}^* \cdot \vec{p}' \vec{S}^* \cdot \vec{p}' \vec{S}^T \cdot \vec{p} \chi_C e^{i\sigma_1} \sqrt{1 + \eta^2} C_\eta}{\sum_{n=0}^N C_{3p}^{(n)} E^n + \frac{y^2}{3\mu^2} \frac{\mu}{2\pi} (2\kappa H_1(p)) + \frac{2y'^2}{15\mu'^4} \frac{\mu'}{2\pi} (ip'^5)}, \end{aligned} \quad (32)$$

where $\Psi_{d\alpha C}^{(3p)}(p)$ is the vertex function of the α - ^{13}C state for $l = 1$ to d_{3p} including the initial Coulomb wavefunction, $D_{3p}(p)$ is the dressed propagator of the resonant $3/2^+$ state of ^{17}O , and $\Gamma_{dnO}^{(3p)}(p')$ is the vertex function of d_{3p} to n - ^{16}O state for $l = 2$. Those three components of the reaction amplitude are presented in Appendix C.

Using the relation in Eq. (16), we define the α and neutron vertices of the $3/2^+$ state as

$$\Gamma_{3p}^\alpha(E) = 2Z_{3p} p W_1(p) C_\eta^2 = \Gamma_{R(3p)}^\alpha \frac{p W_1(p) C_\eta^2}{p_r W_1(p_r) C_{\eta_r}^2}, \quad (33)$$

$$\Gamma_{3p}^n(E) = Z_{3p} \frac{2\mu y'^2}{5\mu'^3 y^2} p'^5 = \Gamma_{R(3p)}^n \left(\frac{E + Q}{E_{R(3p)} + Q} \right)^{5/2}, \quad (34)$$

where Z_{3p} is the wavefunction normalization constant, $\Gamma_{R(3p)}^\alpha$ and $\Gamma_{R(3p)}^n$ are the α and neutron widths, and p_r and η_r are the momentum and Sommerfeld parameter at $E =$

$E_{R(3p)}$. $E_{R(3p)}$ is the resonant energy of the $3/2^+$ state of ^{17}O . Because $\Gamma_{R(3p)}^\alpha$ and $\Gamma_{R(3p)}^n$ are fitted to the experimental data, Z_{3p} can be an arbitrary constant. Thus, we have the reaction amplitude of the $3/2^+$ state as

$$A_{3p} = -\frac{3\pi}{\sqrt{\mu'\mu p'p}} \frac{e^{i\sigma_1} \chi_n^\dagger \vec{\sigma}^* \cdot \hat{p}' \vec{S}^* \cdot \hat{p}' \vec{S}^T \cdot \hat{p} \chi_C \sqrt{\Gamma_{3p}^n(E) \Gamma_{3p}^\alpha(E)}}{E - E_{R(3p)} + R_{3p}(E) + i\frac{1}{2} (\Gamma_{3p}^\alpha(E) + \Gamma_{3p}^n(E))}, \quad (35)$$

where

$$R_{3p}(E) = a_{3p}(E - E_{R(3p)})^2 + b_{3p}(E - E_{R(3p)})^3. \quad (36)$$

The terms in $R_{3p}(E)$ are the higher order terms of the effective range parameters, obtained by Fourier expansion around $E = E_{R(3p)}$. The coefficients, a_{3p} and b_{3p} , describe the shape of the resonant peak and are fitted to the experimental data. To calculate the squared amplitude and angle integral in the phase space, we have

$$\int \frac{d\Omega_{\hat{p}'}}{4\pi} \text{Tr} \left(\vec{S} \cdot \hat{p} \vec{S}^\dagger \cdot \hat{p}' \vec{\sigma}^\dagger \cdot \hat{p}' \vec{\sigma} \cdot \hat{p}' \vec{S} \cdot \hat{p}' \vec{S}^\dagger \cdot \hat{p} \right)^* = \frac{4}{9}, \quad (37)$$

where we have chosen $\hat{p} = (0, 0, 1)$, and we have the expression of the S factor of $^{13}\text{C}(\alpha, n)^{16}\text{O}$ for the $3/2^+$ state of ^{17}O as

$$S_{3p} = \frac{\pi}{\mu} \frac{\Gamma_{3p}^n(E) \Gamma_{3p}^\alpha(E) e^{2\pi\eta}}{\left(E - E_{R(3p)} + R_{3p}(E) \right)^2 + \frac{1}{4} \left(\Gamma_{3p}^n(E) + \Gamma_{3p}^\alpha(E) \right)^2}. \quad (38)$$

The S_{3p} factor has five parameters, $\{E_{R(3p)}, \Gamma_{R(3p)}^n, \Gamma_{R(3p)}^\alpha, a_{3p}, b_{3p}\}$, and they are fitted to the experimental data.

5. Numerical results

In the previous section, we have constructed the S factors of $^{13}\text{C}(\alpha, n)^{16}\text{O}$ for the resonant $1/2^+$, $5/2^-$, $3/2^+$ states of ^{17}O in the cluster EFT. The S factors contain eleven parameters while we fix B as $B = 3$ keV, and the remaining ten parameters, $\{\Gamma_{R(1p)}^n, Z_{1p}, E_{R(5m)}, \Gamma_{R(5m)}^n, \Gamma_{R(5m)}^\alpha, E_{R(3p)}, \Gamma_{R(3p)}^n, \Gamma_{R(3p)}^\alpha, a_{3p}, b_{3p}\}$, are fitted to the experimental data. We employ the data sets of the S factor from Bair and Haas (1973) [23], Drotleff et al. (1993) [24], Heil et al. (2008) [25], LUNA collaboration (2021) [3], JUNA collaboration (2022) [4], and the data for the parameter fit are truncated at the energy $E = 1$ MeV, just below the sharp resonant $5/3^+$ state of ^{17}O . Thus, the energy range of the parameter fit is $E = 0.230$ to 1 MeV, where the data at the smallest energy was reported from the LUNA collaboration. We perform a χ^2 fit in an MCMC analysis by employing the `emcee` package [26]. By using the fitted values of the parameters, we extrapolate the S factor to $E_G = 0.19$ MeV and estimate its error in the MCMC analysis.

Because the resonant energy of the $1/2^+$ state is not covered by the experimental data for the parameter fit, as mentioned before, we fix the resonant energy of the $1/2^+$ state as $E = -B$ where $B = 3$ keV. While the reported neutron width, $\Gamma_{R(1p)}^n = 124(12)$ keV, and the ANC of the $1/2^+$ state of ^{17}O have significant uncertainties, and we do not fix

	10 parameter fit	7 parameter fit	Ref. [21]
$\Gamma_{R(1p)}^n$ (keV)	147_{-83}^{+158}	136_{-100}^{+192}	124(12)*
Z_{1p} (MeV ⁻²)	$3.0_{-1.1}^{+3.3} \times 10^{-3}$	$1.5_{-0.9}^{+2.2} \times 10^{-3}$	
$E_{R(5m)}$ (MeV)	0.806612(17)	—	0.80686(17)
$\Gamma_{R(5m)}^n$ (keV)	2.98(4)	—	1.38(5)*
$\Gamma_{R(5m)}^\alpha$ (eV)	6.32(6)	—	
$E_{R(3p)}$ (MeV)	0.8559(8)	0.8416(15)	0.843(10)
$\Gamma_{R(3p)}^n$ (keV)	285(4)	291(6)	263(7)*
$\Gamma_{R(3p)}^\alpha$ (eV)	99.8(11)	85.8(17)	
a_{3p} (MeV)	1.78(4)	1.32(7)	
b_{3p} (MeV ²)	1.52(13)	$0.51_{-0.14}^{+0.17}$	
χ^2/N (N)	8.20 (216)	0.67 (56)	
$ C_b _{1p}$ (fm ^{-1/2})	$3.16_{-1.16}^{+3.48} \times 10^{90}$	$2.23_{-1.34}^{+3.27} \times 10^{90}$	5.44×10^{90} **
$S(0.19 \text{ MeV})$ (MeV b)	$1.09(11) \times 10^6$	$1.12(8) \times 10^6$	

Table 2: Values of the parameters fitted to the experimental data of the S factor of $^{13}\text{C}(\alpha, n)^{16}\text{O}$ below $E = 1$ MeV. In the second column, the values of ten parameters fitted to the available experimental data are displayed. In the third column, those of the seven parameters fitted to the data reported from the LUNA and JUNA collaborations are presented. In the last column, the values of resonant energies and widths in Ref. [21] are displayed. In the third row from the bottom, values of χ^2/N for the fit where N is the number of data, in the second row from the bottom, those of the ANC of $1/2^+$ state of ^{17}O calculated using the fitted values of Z_{1p} , and in the last row, those of S factor at $E = 0.19$ MeV are displayed. See the text as well. *Total widths, $\Gamma^{tot} \simeq \Gamma_R^n$. **A value found, e.g., in Table II in Ref. [3].

them by using the reported values, but fit the tail from the low-energy pole to the data. We perform two runs of the parameter fit, a ten-parameter fit and a seven-parameter fit. In the first ten-parameter fit, we include all the data sets mentioned above but find a significantly large χ^2 value, $\chi^2/N = 8.20$, where N is the number of data, $N = 216$. In addition, the recently reported data from the JUNA collaboration do not fit well. (See Fig. 3.) In the second seven-parameter fit, we include only the recent two data sets from the LUNA and JUNA collaborations. Because the two data sets do not have the data for the sharp resonant $5/2^-$ state of ^{17}O , we fix the three parameters, $E_{R(5m)}$, $\Gamma_{R(5m)}^n$, $\Gamma_{R(5m)}^\alpha$, by using the values fitted in the first ten parameter fit. The seven parameters $\{\Gamma_{R(1p)}^n, Z_{1p}, E_{R(3p)}, \Gamma_{R(3p)}^n, \Gamma_{R(3p)}^\alpha, a_{3p}, b_{3p}\}$ are fitted to the data.

In Table 2, the fitted values of the parameters in the MCMC analysis are displayed. In the second column of the table, the fitted values of the ten-parameter fit, and in the third column, the fitted values of the seven-parameter fit are presented. In the last column, reference values in the literature are displayed. In the third row from the bottom, the χ^2/N values of the parameter fit are presented, where N is the number of data points. In the second row from the bottom, the values of the ANC of the $1/2^+$ state of ^{17}O at

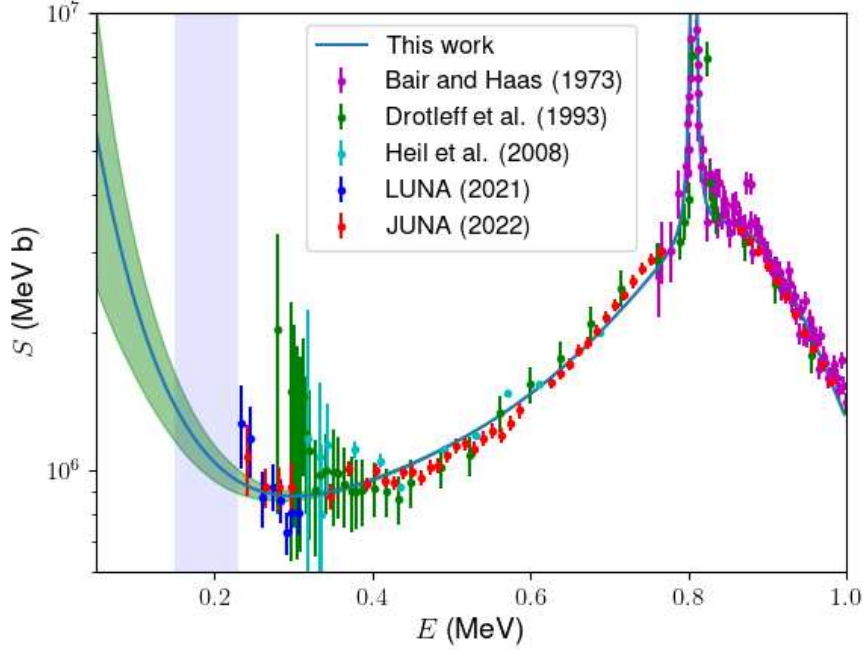


Figure 3: S factor of $^{13}\text{C}(\alpha, n)^{16}\text{O}$ as a function of energy, E , of the initial α - ^{13}C state in the center-of-mass frame. A line is plotted by using fitted values of ten parameters to experimental data, presented in the second column in Table 2. A band of the plotted line is obtained by 16 to 84 % samples of the MCMC analysis. The experimental data are displayed in the figure as well. A vertical band represents a range of the Gamow peak energy in the low mass AGB stars.

$E = -2.69$ keV [5] calculated by using the fitted values of Z_{1p} are displayed. In the last column, the values and errors of the S factor of $^{13}\text{C}(\alpha, n)^{16}\text{O}$ at $E = 0.19$ MeV are presented.

As seen in the table, the fitted values of $\Gamma_{R(1p)}^n$ and Z_{1p} have about 100% error bars, mainly because the experimental data do not cover the energy range for the $1/2^+$ state of ^{17}O . The fitted values of Z_{1p} are converted to the values of the ANC by using Eq. (21), displayed in the second row from the bottom of the table. We find that the fitted values of $\Gamma_{R(1p)}^n$ and $|C_b|_{1p}$ agree with the values in the literature within the large error bars. The fitted value of $E_{R(5m)}$ agrees well that in Ref. [21], while that of $\Gamma_{R(5m)}^n$ is about two times larger. For the parameters for the $3/2^+$ state, two fitted values of $E_{R(3p)}$ agree with that of Ref. [21] within the error bars, while two fitted values of $\Gamma_{R(3p)}^n$ are 8.3% and 10.6% larger than that in Ref. [21].

In Figs. 3 and 4, we plot the S factor of $^{13}\text{C}(\alpha, n)^{16}\text{O}$ as a function of the energy E of the initial α - ^{13}C system in the center-of-mass frame by using the two sets of fitted values of the parameters in Table 2. The green bands of the fitted lines are obtained by 16 to 84 % samples of the MCMC analysis. The experimental data for the parameter fit are

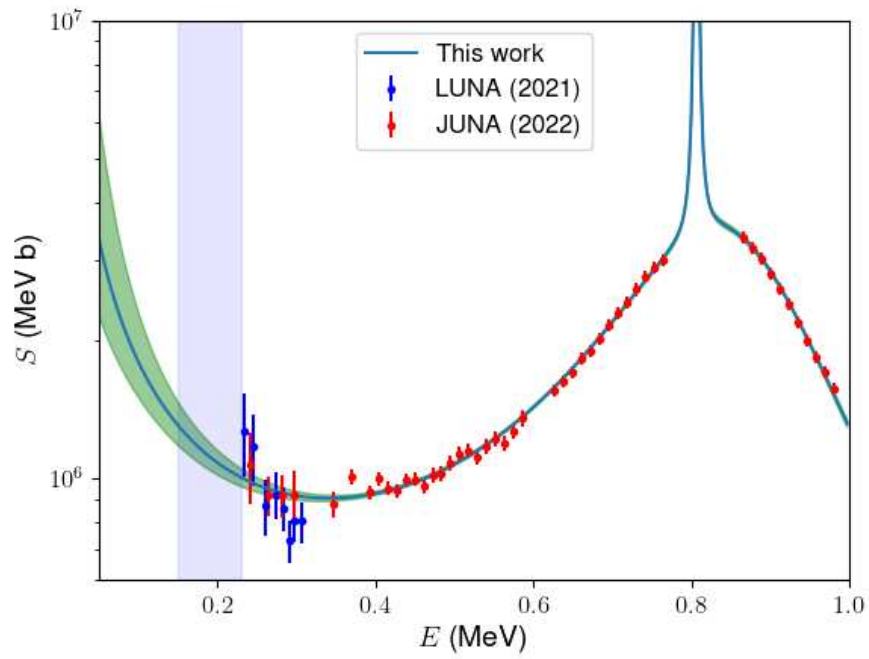


Figure 4: S factor of $^{13}\text{C}(\alpha,n)^{16}\text{O}$ as a function of energy, E , of the initial α - ^{13}C state in the center-of-mass frame. A line is plotted by using fitted values of seven parameters to experimental data of LUNA and JUNA collaborations, presented in the third column in Table 2. See the caption of Fig. 3 as well.

also displayed in the figures. As presented in the table, the χ^2 values of the parameter fit, χ^2/N (N) are 8.20 (216) and 0.67 (56) for the ten and seven parameter fits, respectively. As mentioned above, we have a large χ^2 value in the ten-parameter fit, and one can see that the recent data from JUNA are not well fitted in Fig. 3. In Fig. 4, one can see that the data from LUNA and JUAN are fitted well. Because we do not fix the two parameters, $\Gamma_{R(1p)}^n$ and Z_{1p} , of the $1/2^+$ state by using the values in the literature, the error bands of the S factor increase as the energy E decreases in the vertical band which represents a range of the Gamow peak energy in the low mass AGB stars. In the last row in Table 2, we present our estimate of the S factor at $E_G = 0.19$ MeV. We find that both values of the S factor are in good agreement within the error bars, and we have 10.1% and 7.0% errors in the S factor at E_G .

6. Results and discussion

In the present study, we constructed an EFT for the $^{13}\text{C}(\alpha, n)^{16}\text{O}$ reaction at low energies. We included the resonant $1/2^+$, $5/2^-$, $3/2^+$ states of ^{17}O and the two open channels, α - ^{13}C and n - ^{16}O states, and wrote down an effective Lagrangian for the study. The expressions of the S factors and reaction amplitudes of $^{13}\text{C}(\alpha, n)^{16}\text{O}$ were calculated. We have eleven parameters in the amplitudes, and one of them was fixed by using the resonant energy of the $1/2^+$ state. The remaining parameters were fitted to the data of the S factor at the energies below $E = 1$ MeV. We performed two runs of the parameter fit by employing different sets of the experimental data. By using the fitted values of the parameters, the S factor was extrapolated to $E_G = 0.19$ MeV, and we found that the uncertainties of the S factor are about 10% at E_G . As seen in Figs. 3 and 4, the error bands increase as the energy decreases in the range of the Gamow peak energy in the low mass AGB stars because the parameters, $\Gamma_{R(1p)}^n$ and Z_{1p} , are not fitted well to the experimental data. We confirm, as pointed out in Ref. [5], that the uncertainty of the S factor mainly stems from the near-threshold state of ^{17}O .

The expressions of the S factors of $^{13}\text{C}(\alpha, n)^{16}\text{O}$ obtained in the cluster EFT are almost the same as those in the Breit-Wigner formula. See, e.g., Eq. (2) in Ref. [27]. As pointed out in Ref. [28] for the study of $^3\text{He}(d, n)^4\text{He}$, on one hand, the expression of reaction amplitude calculated in an EFT can be obtained in the limit that the channel radius a sends to zero in an R -matrix analysis. In the present work, on the other hand, we introduced the higher order terms, a_{3p} and b_{3p} , in the effective range expansion in the reaction amplitude for the $3/2^+$ state of ^{17}O . They played a major role in fitting the shape of the S factor at the low-energy side of the resonant $3/2^+$ state without introducing a resonant state at high energy. Some extension in the traditional approach is possible within a framework of EFT.

It was reported that even a factor of $\simeq 4$ uncertainty of $^{13}\text{C}(\alpha, n)^{16}\text{O}$ reaction at $T = 90 \times 10^6$ K gives a negligible influence on models of low-mass AGB stars [29]. So the about 10% uncertainty of the S factor at E_G obtained in this work would be a good estimate of the $^{13}\text{C}(\alpha, n)^{16}\text{O}$ reaction at low energies. While it may also be important to improve the uncertainty of the reaction itself. The values of $\Gamma_{R(1p)}^n$ and Z_{1p} , equivalently the ANC of the $1/2^+$ state of ^{17}O , can be found in the literature, (we listed them in the

tables.) and, as mentioned, we fixed the resonant energy of the $1/2^+$ state as $B = 3$ keV. The resonant $1/2^+$ state has a relatively large width, $\Gamma_{R(3p)}^n = 124(12)$ keV, and the reported value of the resonant energy of the $1/2^+$ state has a relatively large error bar, $B = 3 \pm 8$ keV. Moreover, the ANC is sensitive to the value of B . Thus, we postponed the study of the parameter sets for the $1/2^+$ state of ^{17}O to a future work. To introduce other experimental data, such as elastic n - ^{16}O scattering, in the study may be necessary to fix the parameters of the $1/2^+$ state of ^{16}O and reduce the errors of the S factor of $^{13}\text{C}(\alpha, n)^{16}\text{O}$ at E_G obtained in this work.

Acknowledgements

The author would like to thank Gurgan Adamian for his suggestion to apply a cluster EFT to the study of nuclear reactions, Chang Ho Hyun and Ki-Seok Choi for discussions in the early stage of the work, and Jubin Park for discussions about the R -matrix analysis. This work was supported by the National Research Foundation grant funded by the Korean government Ministry of Science and ICT (Grants No. 2023R1A2C1003177 and No. RS-2025-16065411).

References

- [1] O. Straniero, R. Gallino, S. Cristallo, s process in low-mass asymptotic giant stars, *Nucl. Phys. A* **777**, 311 (2006).
- [2] C. Sneden, J. J. Cowan, R. Gallino, Neutron-capture elements in the early galaxy, *Annu. Rev. Astron. Astrophys.* **46**, 241 (2008).
- [3] G. F. Ciani et al. (LUNA Collaboration), Direct measurement of the $^{13}\text{C}(\alpha, n)^{16}\text{O}$ cross section into the s -process Gamow peak, *Phys. Rev. Lett.* **127**, 152701 (2021).
- [4] B. Gao et al. (JUNA Collaboration), Deep underground laboratory measurement of $^{13}\text{C}(\alpha, n)^{16}\text{O}$ in the Gamow windows of the s and i processes, *Phys. Rev. Lett.* **129**, 132701 (2022).
- [5] R. J. deBoer et al., Sensitivity of the $^{13}\text{C}(\alpha, n)^{16}\text{O}$ S factor to the uncertainty in the level parameters of the near-threshold state, *Phys. Rev. C* **101**, 045802 (2020).
- [6] S. Weinberg, Phenomenological lagrangians, *Physica A* **79**, 327 (1979).
- [7] J. F. Donoghue, E. Golowich, B. R. Holstein, *Dynamics of the Standard Model* (Second Edition, Cambridge University Press, 2014).
- [8] S.-I. Ando, Elastic α - ^{12}C scattering at low energies in cluster effective field theory, *Eur. Phys. J. A* **52**, 130 (2016)
- [9] S.-I. Ando, Elastic α - ^{12}C scattering at low energies with the bound states of ^{16}O in effective field theory, *Phys. Rev. C* **97**, 014604 (2018).

- [10] S.-I. Ando, S matrices of elastic α - ^{12}C scattering at low energies in effective field theory, *Phys. Rev. C* **107**, 045808 (2023).
- [11] M.-H. Mun, J. Park, C. H. Hyun, S.-I. Ando, Analysis of elastic α - ^{12}C scattering with machine learning in the cluster effective field theory, arXiv:2511.06382 (2025), accepted for publication in *Phys. Rev. C*.
- [12] S.-I. Ando, Cluster effective field theory and nuclear reactions, *Eur. Phys. J. A* **57**, 17 (2021)
- [13] S.-I. Ando, The S_{E1} factor of radiative α capture on ^{12}C in cluster effective field theory, *Phys. Rev. C* **100**, 015807 (2019).
- [14] S.-I. Ando, Fixing effective range parameters in elastic α - ^{12}C scattering: an impact on resonance 2_4^+ state of ^{16}O and S_{E2} factor of $^{12}\text{C}(\alpha,\gamma)^{16}\text{O}$, *Chinese Phys. C* **49**, 094107 (2025).
- [15] S.-I. Ando, Radiative α capture on ^{12}C in cluster effective field theory: short review, *Nucl. Phys. A* **1060**, 123108 (2025).
- [16] J. B. Habashi, S. Fleming, U. van Kolck, Nonrelativistic effective field theory with a resonance field, *Euro. Phys. J. A* **57**, 169 (2021).
- [17] D. B. Kaplan, More effective field theory for nonrelativistic scattering, *Nucl. Phys. B* **494**, 471 (1997).
- [18] S. R. Beane and M. J. Savage, Rearranging pionless effective field theory, *Nucl. Phys. A* **694**, 511 (2001).
- [19] S.-I. Ando and C. H. Hyun, Effective field theory of the deuteron with dibaryon field, *Phys. Rev. C* **72**, 014008 (2005).
- [20] L. Fernando, R. Higa, and G. Rupak, Leading E1 and M1 contributions to radiative neutron capture on lithium-7, *Eur. Phys. J. A* **48**, 24 (2012)
- [21] D. R. Tilley, H. R. Weller, C. M. Cheves, Energy levels of light nuclei $A = 16$ – 17 , *Nucl. Phys. A* **564**, 1 (1993).
- [22] Z. R. Iwinski, L. Rosenberg, L. Spruch, Radiative capture estimates via analytic continuation of elastic-scattering data, and solar-neutrino problem, *Phys. Rev. C* **29**, 349(R) (1984).
- [23] J. K. Bair and F. X. Haas, Total neutron yield from the reactions $^{13}\text{C}(\alpha,n)^{16}\text{O}$ and $^{17,18}\text{O}(\alpha,n)^{20,21}\text{Ne}$, *Phys. Rev. C* **7**, 1356 (1973).
- [24] H. W. Drotleff et al., Reaction rates of the s -process neutron sources $^{22}\text{Ne}(\alpha,n)^{25}\text{Mg}$ and $^{13}\text{C}(\alpha,n)^{16}\text{O}$, *Astrophys. J.* **414**, 735 (1993).

- [25] M. Heil et al., The $^{13}\text{C}(\alpha, n)^{16}\text{O}$ reaction and its role as a neutron source for the s process, Phys. Rev. C **78**, 025803 (2008).
- [26] D. Foreman-Mackey, D. W. Hogg, D. Lang, J. Goodman, **emcee**: The MCMC Hammer, Publ. Astron. Soc. Pac. **125**, 306 (2013).
- [27] B. Guo et al., New determination of the $^{13}\text{C}(\alpha, n)^{16}\text{O}$ reaction rate and its influence on the s -process nucleosynthesis in AGB stars, Astr. J. **756**, 193 (2012)
- [28] G. M. Hale, L. S. Brown, M. W. Paris, Effective field theory as a limit of R -matrix theory for light nuclear reactions, Phys. Rev. C **89**, 014623 (2014).
- [29] S. Cristallo, O. Straniero, R. Gallino, S -process nucleosynthesis in low mass AGB stars: do we really need an improved determination of the $^{13}\text{C}(\alpha, n)^{16}\text{O}$ rate?, Nucl. Phys. A **758**, 509c (2005).
- [30] J. J. Sakurai, Modern Quantum Mechanics, Cambridge University Press (2021)

Appendix A: Projection operators

In this appendix, we present the expressions of the matrices, S_i , L_i , R_i , and discuss the projection operators in Eqs. (8) and (9). The expression of the operator $P_{1/2}^{(l=0)}$ is obvious, $P_{1/2}^{(l=0)} = 1$, for the n - ^{16}O channel with $l = 0$ and spin-1/2 states.

- $P_{1/2, i}^{(l=1)}$; $J^\pi = 1/2^+$ state for the α - ^{13}C channel with $l = 1$ and spin-1/2 states

For the term with the y_{1p} coefficient in Eq. (68), in the center-of-mass frame, we choose the momentum of light particle α (n) as $+\vec{p}$ and that of heavy particle ^{13}C (^{16}O) as $-\vec{p}$, and the projection operator, $O_i^{(l=1)}$, leads to $p_i/\mu_{\alpha C}$ where $\mu_{\alpha O}$ is the reduced mass of α and ^{13}C (p_i/μ_{nO} for the n - ^{16}O channel where μ_{nO} is the reduced mass of n and ^{16}O). Thus one has

$$d_{1p}^\dagger \left(P_{1/2, i}^{(l=1)} \psi_{13C} O_i^{(l=1)} \phi_\alpha \right) \rightarrow \frac{1}{\mu_{\alpha C}} \chi_{1p}^\dagger \left(-\frac{1}{\sqrt{3}} \vec{\sigma}^T \cdot \vec{p} \right) \chi_C, \quad (39)$$

where χ_{1p} and χ_C are the two-component spinors of the $1/2^+$ state of ^{17}O and ^{13}C , respectively. Using the relations of the Cartesian tensors [30],

$$\hat{p}_\pm = \mp \frac{1}{\sqrt{2}} (\hat{p}_1 \pm i\hat{p}_2), \quad \sigma_\pm = \frac{1}{2} (\sigma_1 \pm i\sigma_2), \quad (40)$$

and $p_z = p_0$ and $\sigma_3 = \sigma_0$, one has

$$\vec{\sigma} \cdot \hat{p} = -\sqrt{2}\sigma_- \hat{p}_+ + \sqrt{2}\sigma_+ \hat{p}_- + \sigma_0 \hat{p}_0 = \begin{pmatrix} \hat{p}_0 & \sqrt{2}\hat{p}_- \\ -\sqrt{2}\hat{p}_+ & -\hat{p}_0 \end{pmatrix}, \quad (41)$$

where $\sigma_\pm^\dagger = \sigma_\mp$ and $\hat{p}_\pm^* = -\hat{p}_\mp$. It leads to

$$\chi^{J=1/2} = -\frac{1}{\sqrt{3}} \vec{\sigma}^T \cdot \hat{p} \chi_C, \quad (42)$$

with $\chi_C^T = (\chi_C^+, \chi_C^-)$, and

$$\chi_{(J=1/2)}^+ = \sqrt{\frac{2}{3}}\hat{p}_+\chi_C^- - \frac{1}{\sqrt{3}}\hat{p}_-\chi_C^+, \quad \chi_{(J=1/2)}^- = -\sqrt{\frac{2}{3}}\hat{p}_-\chi_C^+ + \frac{1}{\sqrt{3}}\hat{p}_0\chi_C^-, \quad (43)$$

where one can see that the Clebsch-Gordan coefficients of spin 1/2 state from $1 \otimes \frac{1}{2}$ spin states are reproduced.

- $P_{3/2,i}^{(l=1)}$; $J^\pi = 3/2^+$ state for the α - ^{13}C channel with $l = 1$ state and spin-1/2 state
We employ the transition matrices from spin-1/2 to spin-3/2 [20],

$$\begin{aligned} S_1 &= \frac{1}{\sqrt{6}} \begin{pmatrix} -\sqrt{3} & 0 & 1 & 0 \\ 0 & -1 & 0 & \sqrt{3} \end{pmatrix}, \quad S_2 = -\frac{i}{\sqrt{6}} \begin{pmatrix} \sqrt{3} & 0 & 1 & 0 \\ 0 & 1 & 0 & \sqrt{3} \end{pmatrix}, \\ S_3 &= \sqrt{\frac{2}{3}} \begin{pmatrix} 0 & 1 & 0 & 0 \\ 0 & 0 & 1 & 0 \end{pmatrix}, \end{aligned} \quad (44)$$

with

$$S_i S_j^\dagger = \frac{2}{3}\delta_{ij} - i\frac{1}{3}\epsilon_{ijk}\sigma_k, \quad \vec{\sigma} \cdot \vec{S} = 0. \quad (45)$$

These matrices may be rewritten as

$$S_\pm = \frac{1}{2}(S_1 \pm iS_2), \quad S_0 = S_3 \quad (46)$$

where

$$S_+ = \frac{1}{\sqrt{6}} \begin{pmatrix} 0 & 0 & 1 & 0 \\ 0 & 0 & 0 & \sqrt{3} \end{pmatrix}, \quad S_- = -\frac{1}{\sqrt{6}} \begin{pmatrix} 0 & 1 & 0 & 0 \\ \sqrt{3} & 0 & 0 & 0 \end{pmatrix}, \quad (47)$$

and one has

$$\begin{aligned} \vec{S} \cdot \hat{l} &= \sqrt{2}\hat{l}_-S_+ - \sqrt{2}\hat{l}_+S_+ + \hat{l}_0S_0 \\ &= \frac{1}{\sqrt{3}} \begin{pmatrix} \sqrt{3}\hat{l}_+ & \sqrt{2}\hat{l}_0 & \hat{l}_- & 0 \\ 0 & \hat{l}_+ & \sqrt{2}\hat{l}_0 & \sqrt{3}\hat{l}_- \end{pmatrix}, \end{aligned} \quad (48)$$

where \hat{l} is a unit vector, and a vector \vec{l} is obtained from the angular momentum projection operator for $l = 1$. Now a $J = 3/2$ state generated from $l = 1$ and $s = 1/2$ is obtained as

$$\chi_m^{(J=3/2)} = \vec{S}^T \cdot \hat{l} \chi_C, \quad (49)$$

where $m = \pm 3/2, \pm 1/2$ and

$$\begin{aligned} \chi_{+3/2}^{(J=3/2)} &= \hat{l}_+\chi_C^+, \quad \chi_{+1/2}^{(J=3/2)} = \frac{1}{\sqrt{3}}\hat{l}_+\chi_C^- + \sqrt{\frac{2}{3}}\hat{l}_0\chi_C^+, \\ \chi_{-1/2}^{(J=3/2)} &= \frac{1}{\sqrt{3}}\hat{l}_-\chi_C^+ + \sqrt{\frac{2}{3}}\hat{l}_0\chi_C^-, \quad \chi_{-3/2}^{(J=3/2)} = \hat{l}_-\chi_C^-, \end{aligned} \quad (50)$$

where one can see that the Clebsch-Gordan coefficients of spin 3/2 state from $1 \otimes \frac{1}{2}$ spin states are reproduced.

- $P_{3/2,ij}^{(l=2)}$; $J^\pi = 3/2^+$ state for the $n\text{-}^{16}\text{O}$ system with $l = 2$ and spin-1/2 states

A naive expectation to construct a projection operator for $J = 3/2$ state from $l = 2$ and spin-1/2 states is to replace the spin-1/2 state to the $J = 1/2$ state from $l = 1$ and spin-1/2 states in the $P_{3/2,i}^{(l=1)}$ operator, $\vec{S}^T \cdot \vec{l}\chi_n \rightarrow \vec{S}^T \cdot \vec{l}(-1/\sqrt{3})\vec{\sigma}^T \cdot \vec{l}\chi_n$. To reproduce the Clebsch-Gordan coefficients of the spin 3/2 state from $2 \otimes \frac{1}{2}$ states, the overall coefficients should be modified. Thus, we have

$$\chi_m^{(J=3/2)} = -\sqrt{\frac{2}{5}}\vec{S}^T \cdot \hat{l}\vec{\sigma}^T \cdot \hat{l}\chi_n. \quad (51)$$

Employing the expressions of the Cartesian tensor of rank 2 [30],

$$\begin{aligned} T_{\pm 2}^{(2)} &= U_{\pm 1}V_{\pm 1} = \hat{l}_{\pm}\hat{l}_{\pm}, & T_{\pm 1}^{(2)} &= \frac{1}{\sqrt{2}}(U_{\pm 1}V_0 + U_0V_{\pm 1}) = \sqrt{2}\hat{l}_0\hat{l}_{\pm}, \\ T_0^{(2)} &= \frac{1}{\sqrt{6}}(U_{+1}V_{-1} + 2U_0V_0 + U_{-1}V_{+1}) = \sqrt{\frac{2}{3}}(\hat{l}_+\hat{l}_- + \hat{l}_0\hat{l}_0), \end{aligned} \quad (52)$$

where vectors \vec{l} are generated from the angular momentum operator for $l = 2$. Thus, we have

$$\begin{aligned} \chi_{+3/2}^{(J=3/2)} &= \sqrt{\frac{4}{5}}T_{+2}^{(2)}\chi_-^s - \frac{1}{\sqrt{5}}T_{+1}^{(2)}\chi_+^s, & \chi_{+1/2}^{(J=3/2)} &= \sqrt{\frac{3}{5}}T_{+1}^{(2)}\chi_-^s - \sqrt{\frac{2}{5}}T_0^{(2)}\chi_+^s, \\ \chi_{-1/2}^{(J=3/2)} &= \sqrt{\frac{2}{5}}T_0^{(2)}\chi_-^s - \sqrt{\frac{3}{5}}T_{-1}^{(2)}\chi_+^s, & \chi_{-3/2}^{(J=3/2)} &= \frac{1}{\sqrt{5}}T_{-1}^{(2)}\chi_-^s - \sqrt{\frac{4}{5}}T_{-2}^{(2)}\chi_+^s, \end{aligned} \quad (53)$$

where one can see that the Clebsch-Gordan coefficients of spin 3/2 state from $2 \otimes \frac{1}{2}$ spin states are reproduced.

- $P_{5/2,ij}^{(l=2)}$; $J^\pi = 5/2^-$ state for the $\alpha\text{-}^{13}\text{C}$ channel with $l = 2$ and spin-1/2 states

The spin $5/2^-$ state from the $l = 2$ and spin-1/2 state is constructed as spin-angular functions ⁵, and we have

$$\frac{1}{\sqrt{5}}M^T\chi_C, \quad (54)$$

where M is a 2×6 matrix,

$$M = \begin{pmatrix} \sqrt{5}T_{22} & \sqrt{4}T_{21} & \sqrt{3}T_{20} & \sqrt{2}T_{2-1} & T_{2-2} & 0 \\ 0 & T_{22} & \sqrt{2}T_{21} & \sqrt{3}T_{20} & \sqrt{4}T_{2-1} & \sqrt{5}T_{2-2} \end{pmatrix}, \quad (55)$$

⁵See Eq. (3.7.64) in Ref. [30]. We note that S_i matrices in Eq. (44) can be constructed in the same way.

$$R_3 = \begin{pmatrix} 0 & 2 & 0 & & & \\ & 0 & \sqrt{2} & 0 & & \\ & & 0 & \sqrt{2} & 0 & \\ & & & 0 & 2 & 0 \end{pmatrix}. \quad (64)$$

Here, the blank spaces in the R matrices represent zero elements. We also have relations,

$$\vec{\sigma} \cdot \vec{L} = 0, \quad \vec{L} \cdot \vec{R} = 0, \quad \vec{\sigma} \cdot L_a \vec{R} = 0, \quad (65)$$

where $a = 1, 2, 3$.

- $P_{5/2,ijk}^{(l=3)}$: $J^\pi = 5/2^-$ state for the n - ^{16}O channel with $l = 3$ and spin-1/2 states

We construct the projection operator of $J = 5/2$ from $l = 3$ and spin-1/2 states by imposing a naive expectation. We replace the 1/2-spinor acting on $P_{5/2,ij}^{(l=2)}$ by $P_{1/2,k}^{(l=1)} \chi_n$, and have

$$-\frac{1}{\sqrt{15}} R_i^T L_j^T \sigma_k^T \chi_n. \quad (66)$$

We note that this expression does not reproduce the terms and coefficients of the expression of the $J = 5/2$ state from $3 \otimes \frac{1}{2}$ spin states in terms of the Clebsch-Gordan coefficients. In the present work, an overall factor of the operator can be arbitrary due to the definitions of the neutron width, $\Gamma_{R(5m)}^n$. An arbitrary normalization factor C of the projection operator, $P_{5/2,ijk}^{(l=3)}$, may appear from the vertex function $\Gamma_{dnO}^{(5m)}(p)$, and it is absorbed in $\sqrt{\Gamma_{R(5m)}^n}$ in the numerator of the reaction amplitude. Another arbitrary factor C^2 may appear from the self-energy, $\Sigma_{nO}^{(5m)}(p)$, and it is absorbed in $\Gamma_{R(5m)}^n$ in the denominator. The neutron width, $\Gamma_{R(5m)}^n$, should be fitted by experimental data. We also confirm that by using the projection operator in Eq. (66), the overall factor of the S factor of the Breit-Wigner formula ⁶ is reproduced.

Appendix B: Angular momentum projection operators

In this appendix, we display the expressions of the project operators of the cluster states in the relative angular momenta with $l = 0, 1, 2, 3$ [8, 12]. For the α - ^{13}C system, the angular momentum projection operators, $O_i^{(l=1)}$ and $O_{ij}^{(l=2)}$ for $l = 1$ and $l = 2$, respectively, are given by

$$O_i^{(l=1)} = +i \left(\frac{\overleftarrow{\nabla}}{m_{13C}} - \frac{\overrightarrow{\nabla}}{m_\alpha} \right)_i, \quad O_{ij}^{(l=2)} = O_{ij}^{(\alpha C)} - \frac{1}{3} \delta_{ij} O_{kk}^{(\alpha C)}, \quad (67)$$

with

$$O_{ij}^{(\alpha C)} = \left(i \frac{\overleftarrow{\nabla}}{m_{13C}} \right)_i \left(i \frac{\overleftarrow{\nabla}}{m_{13C}} \right)_j - 2 \left(i \frac{\overleftarrow{\nabla}}{m_{13C}} \right)_i \left(i \frac{\overrightarrow{\nabla}}{m_\alpha} \right)_j + \left(i \frac{\overleftarrow{\nabla}}{m_\alpha} \right)_i \left(i \frac{\overrightarrow{\nabla}}{m_\alpha} \right)_j. \quad (68)$$

⁶See, e.g., Eq. (2) in Ref. [27].

The angular momentum projection operators of the n - ^{16}O system for $l = 0, 2, 3$ are given by

$$\begin{aligned} O^{(l=0)} &= 1, \quad O_{ij}^{(l=2)} = O_{ij}^{(nO)} - \frac{1}{3}\delta_{ij}O_{kk}^{(nO)}, \\ O_{ijk}^{(l=3)} &= O_{ijk}^{(nO)} - \frac{1}{5}\left(\delta_{ij}O_{kl}^{(nO)} + \delta_{ik}O_{jl}^{(nO)} + \delta_{jk}O_{il}^{(nO)}\right), \end{aligned} \quad (69)$$

with

$$O_{ij}^{(nO)} = \left(i\frac{\vec{\nabla}}{m_O}\right)_i \left(i\frac{\vec{\nabla}}{m_O}\right)_j - 2\left(i\frac{\vec{\nabla}}{m_O}\right)_i \left(i\frac{\vec{\nabla}}{m_n}\right)_j + \left(i\frac{\vec{\nabla}}{m_n}\right)_i \left(i\frac{\vec{\nabla}}{m_n}\right)_j, \quad (70)$$

$$\begin{aligned} O_{ijk}^{(nO)} &= \left(i\frac{\vec{\nabla}}{m_O}\right)_i \left(i\frac{\vec{\nabla}}{m_O}\right)_j \left(i\frac{\vec{\nabla}}{m_O}\right)_k - 3\left(i\frac{\vec{\nabla}}{m_O}\right)_i \left(i\frac{\vec{\nabla}}{m_O}\right)_j \left(i\frac{\vec{\nabla}}{m_n}\right)_k \\ &+ 3\left(i\frac{\vec{\nabla}}{m_O}\right)_i \left(i\frac{\vec{\nabla}}{m_n}\right)_j \left(i\frac{\vec{\nabla}}{m_n}\right)_k - \left(i\frac{\vec{\nabla}}{m_n}\right)_i \left(i\frac{\vec{\nabla}}{m_n}\right)_j \left(i\frac{\vec{\nabla}}{m_n}\right)_k. \end{aligned} \quad (71)$$

Appendix C: Propagators, vertices, and self-energies

In this appendix, we display and discuss the expressions of bare propagators, vertices, self-energies, and dressed propagators calculated from the effective Lagrangian. Except for the expressions of the bare propagators, the components are calculated in the center-of-mass frame. The reaction amplitudes of the three resonant states of ^{17}O are calculated by combining those components.

C.1 Bare propagators

The inverse of propagators for n , ^{16}O , α , ^{13}C fields are represented in terms of the standard non-relativistic form, which are obtained from the effective Lagrangian, \mathcal{L}_0 in Eq. (5), as

$$D_P(p_0, \vec{p})^{-1} = p_0 - \frac{1}{2m_P}\vec{p}^2 + i\epsilon, \quad (72)$$

where P represent particles, $P = n, ^{16}\text{O}, \alpha, ^{13}\text{C}$.

The inverse of bare propagators for the resonant $1/2^+$, $5/2^-$, $3/2^+$ states of ^{17}O are obtained from the effective Lagrangian, \mathcal{L}_R in Eq. (6), as

$$\mathring{D}_S(p_0, \vec{p})^{-1} = \sum_{n=0}^N C_S^{(n)} \left(p_0 - \frac{1}{2m_S}\vec{p}^2 + i\epsilon\right)^n, \quad (73)$$

where S represents resonant states, $S = 1p, 5m, 3p$. In this work, we choose the number of terms for the perturbative expansion as $N = 1$ for the $1/2^+$ and $5/2^-$ states and $N = 3$ for the $3/2^+$ state of ^{17}O . We note that, when one chooses the center-of-mass frame, the total three momenta vanish, $\vec{p} = 0$, and the expansion becomes a power series of the energy, $p_0^n = E^n$.

C.2 Vertices

The d - n - ^{16}O vertices for the three resonant states are obtained from the effective Lagrangian, \mathcal{L}_{int} in Eq. (7), as

$$\Gamma_{dnO}^{(1p)} = -y'_{1p}\chi_n^\dagger, \quad (74)$$

$$\Gamma_{dnO}^{(5m)} = \frac{1}{\sqrt{15}} \frac{y'_{5m}}{\mu_{nO}^3} \chi_n^\dagger \sigma_a^* L_b^* R_c^* \mathcal{O}_{abc}^{(l=3)}, \quad (75)$$

$$\Gamma_{dnO}^{(3p)} = \sqrt{\frac{2}{5}} \frac{y'_{3p}}{\mu_{nO}^2} \chi_n^\dagger \vec{\sigma}^* \cdot \vec{l} \vec{S}^* \cdot \vec{l}, \quad (76)$$

with

$$\mathcal{O}_{abc}^{(l=3)} = l_a l_b l_c - \frac{1}{5} (\delta_{ab} l_c + \delta_{ac} l_b + \delta_{bc} l_a) l^2, \quad (77)$$

and l_a is the relative momentum of n and ^{16}O .

The d - α - ^{12}C vertices for the three resonant states are obtained from the effective Lagrangian, \mathcal{L}_{int} in Eq. (7), as

$$\Gamma_{d\alpha C}^{(1p)} = \frac{y_{1p}}{\sqrt{3}\mu_{\alpha C}} \vec{\sigma}^T \cdot \vec{l} \chi_C, \quad (78)$$

$$\Gamma_{d\alpha C}^{(5m)} = -\frac{y_{5m}}{\sqrt{5}\mu_{\alpha C}^2} \vec{R}^T \cdot \vec{l} \vec{L}^T \cdot \vec{l} \chi_C, \quad (79)$$

$$\Gamma_{d\alpha C}^{(3p)} = -\frac{y_{3p}}{\mu_{\alpha C}} \vec{S}^T \cdot \vec{l} \chi_C, \quad (80)$$

where \vec{l} is the relative momentum of α and ^{13}C . When we include the initial Coulomb wavefunctions for $l = 1$ and $l = 2$ [12], the vertex functions are obtained as

$$\Psi_{d\alpha C}^{(1p)}(p) = \frac{y_{1p}}{\sqrt{3}\mu_{\alpha C}} \vec{\sigma}^T \cdot \vec{p} \chi_C e^{i\sigma_1} C_\eta \sqrt{1 + \eta^2}, \quad (81)$$

$$\Psi_{d\alpha C}^{(5m)}(p) = -\frac{y_{5m}}{2\sqrt{5}\mu_{\alpha C}^2} \vec{R}^T \cdot \vec{p} \vec{L}^T \cdot \vec{p} \chi_C e^{i\sigma_2} \sqrt{(1 + \eta^2)(4 + \eta^2)} C_\eta, \quad (82)$$

$$\Psi_{d\alpha C}^{(3p)}(p) = -\frac{y_{3p}}{\mu_{\alpha C}} \vec{S}^T \cdot \vec{p} \chi_C e^{i\sigma_1} \sqrt{1 + \eta^2} C_\eta, \quad (83)$$

with

$$C_\eta = \sqrt{\frac{2\pi\eta}{e^{2\pi\eta} - 1}}, \quad (84)$$

where $p = |\vec{p}|$; \vec{p} is the relative momentum of α and ^{13}C . η is the Sommerfeld parameter, $\eta = \kappa/p$ where κ is the inverse of the Bohr radius of the α - ^{13}C system. σ_1 and σ_2 are the Coulomb phase shifts for $l = 1$ and $l = 2$, respectively.

C.3 Self-energies

- $n\text{-}^{16}\text{O}$ loops

The self-energy term from the one-loop diagram of $n\text{-}^{16}\text{O}$ for the $1/2^+$ state is calculated as

$$\begin{aligned} i\Sigma_{nO}^{(1p)}(p) &= (-iy'_{1p})^2 \int \frac{d^4l}{(2\pi)^4} \frac{i}{l_0 + p_0 - \frac{1}{2m_n}(\vec{l} + \vec{p})^2 + i\epsilon} \frac{i}{-l_0 - \frac{1}{2m_O}\vec{l}^2 + i\epsilon} \\ &= 2i\mu_{nO}y_{1p}^2 \int \frac{d^3\vec{l}}{(2\pi)^3} \frac{1}{\vec{l}^2 + D'}, \end{aligned} \quad (85)$$

where

$$D' = -2\mu_{nO}(E + Q) - i\epsilon = -p'^2 - i\epsilon. \quad (86)$$

The loop integral in Eq. (85),

$$I = \int \frac{d^3\vec{l}}{(2\pi)^3} \frac{1}{\vec{l}^2 + D'} = \frac{1}{2\pi^2} \left(\int_0^\infty dl - \frac{\pi}{2} \sqrt{D'} \right), \quad (87)$$

has a linear divergence, and it is renormalized by the term, $C_{1p}^{(0)}$. The finite part of the self-energy of the $n\text{-}^{16}\text{O}$ loop for the $1/2^+$ state is obtained as

$$\Sigma_{nO}^{(1p)}(p) = -y_{1p}^2 \frac{\mu_{nO}}{2\pi} \sqrt{D'} = +y_{1p}^2 \frac{\mu_{nO}}{2\pi} (ip'). \quad (88)$$

The self-energy term from the $n\text{-}^{16}\text{O}$ loop for the $5/2^-$ state is

$$\begin{aligned} i\Sigma_{nO}^{(5m)}(p) &= i^4 \frac{1}{15} \frac{y_{5m}^2}{\mu_{nO}^6} \int \frac{d^4l}{(2\pi)^4} \frac{R_a^T L_b^T \sigma_c^T \sigma_i^* L_j^* R_k^* \hat{O}_{abc}^{(l=3)} \hat{O}_{ijk}^{(l=3)}}{(l_0 + E + Q - \frac{1}{2m_n}\vec{l}^2 + i\epsilon)(-l_0 - \frac{1}{2m_O}\vec{l}^2 + i\epsilon)} \\ &= i \frac{y_{5m}^2}{15\mu_{nO}^6} \frac{2\mu_{nO}}{2\pi^2} \int_0^\infty dl \frac{l^8}{l^2 + D'} \int \frac{d\Omega_{\hat{l}}}{4\pi} R_a^T L_b^T \sigma_c^T \sigma_i^* L_j^* R_k^* \hat{O}_{abc}^{(l=3)} \hat{O}_{ijk}^{(l=3)}, \end{aligned} \quad (89)$$

where

$$\hat{O}_{abc}^{(l=3)} = \hat{l}_a \hat{l}_b \hat{l}_c - \frac{1}{5} (\delta_{ab} \hat{l}_c + \delta_{ac} \hat{l}_b + \delta_{bc} \hat{l}_a), \quad (90)$$

and

$$\int_0^\infty dl \frac{l^8}{l^2 + D'} = \int_0^\infty dl \left(l^6 - D'l^4 + D'^2 l^2 - D'^3 + \frac{D'^4}{l^2 + D'} \right), \quad (91)$$

and the four divergent terms are renormalized by the terms, $C_{5m}^{(3)}$, $C_{5m}^{(2)}$, $C_{5m}^{(1)}$, $C_{5m}^{(0)}$, and the finite part of the integral is obtained as

$$\int_0^\infty dl \frac{D'^4}{l^2 + D'} = \frac{\pi}{2} D'^{7/2}. \quad (92)$$

The angle integral is calculated as

$$\int \frac{d\Omega_{\hat{l}}}{4\pi} R_a^\dagger L_b^\dagger \sigma_c^\dagger \sigma_d L_e R_f \hat{O}_{abc}^{(l=3)} \hat{O}_{def}^{(l=3)} = \frac{2}{3} I_{6 \times 6}, \quad (93)$$

where $I_{6 \times 6}$ is the 6×6 unit matrix, and we have the finite part of the self-energy of the $n^{-16}\text{O}$ loop for the $5/2^-$ state as

$$\Sigma_{nO}^{(5m)}(p) = \frac{2y_{5m}^2 \mu_{nO}}{45\mu_{nO}^6} \frac{\mu_{nO}}{2\pi} D'^{7/2} = \frac{2y_{5m}^2 \mu_{nO}}{45\mu_{nO}^6} \frac{\mu_{nO}}{2\pi} (ip'^7). \quad (94)$$

The self-energy from the $n^{-16}\text{O}$ loop for the $3/2^+$ state is

$$i\Sigma_{nO}^{(3p)}(p) = +i\frac{2}{5} \frac{\mu_{3p}^2}{\mu_{nO}^4} (2\mu_{nO}) \int \frac{d^3\vec{l}}{(2\pi)^3} \frac{\vec{S}^T \cdot \vec{l} \vec{\sigma}^T \cdot \vec{l} \vec{\sigma}^* \cdot \vec{l} \vec{S}^* \cdot \vec{l}}{\vec{l}^2 + D'}, \quad (95)$$

and the integral in the self-energy term is calculated as

$$\begin{aligned} I &= \int \frac{d^3\vec{l}}{(2\pi)^3} \frac{\vec{S}^T \cdot \vec{l} \vec{\sigma}^T \cdot \vec{l} \vec{\sigma}^* \cdot \vec{l} \vec{S}^* \cdot \vec{l}}{\vec{l}^2 + D'} \\ &= \frac{1}{2\pi^2} \int_0^\infty dl \frac{l^6}{l^2 + D'} \int \frac{d\Omega_{\hat{l}}}{4\pi} \vec{S}^T \cdot \hat{l} \vec{\sigma}^T \cdot \hat{l} \vec{\sigma}^* \cdot \hat{l} \vec{S}^* \cdot \hat{l}, \end{aligned} \quad (96)$$

where the part of the momentum integral leads to

$$I_l = \int_0^\infty dl \frac{l^6}{l^2 + D'} = \int_0^\infty dl \left(l^4 - D'l^2 + D'^2 - \frac{D'^3}{l^2 + D'} \right). \quad (97)$$

The three divergent terms are renormalized by the terms, $C_{3m}^{(2)}$, $C_{3m}^{(1)}$, $C_{3m}^{(0)}$, and the finite part is obtained as

$$I_l^{fin} = -\frac{\pi}{2} D'^{5/2}. \quad (98)$$

By using the relation of the angle integral

$$\int \frac{d\Omega_{\hat{l}}}{4\pi} \hat{l}_a \hat{l}_b \hat{l}_c \hat{l}_d = \frac{1}{15} (\delta_{ab}\delta_{cd} + \delta_{ac}\delta_{bd} + \delta_{ad}\delta_{bc}), \quad (99)$$

one has

$$\begin{aligned} I_i &= \int \frac{d\Omega_{\hat{l}}}{4\pi} \vec{S}^T \cdot \hat{l} \vec{\sigma}^T \cdot \hat{l} \vec{\sigma}^* \cdot \hat{l} \vec{S}^* \cdot \hat{l} = \frac{1}{15} \left(\vec{S}^T \cdot \vec{\sigma}^\dagger \vec{\sigma} \cdot \vec{S} + S_i^\dagger \sigma_j^\dagger \sigma_i S_j + S_i^\dagger \sigma_j^\dagger \sigma_j S_i \right)^* \\ &= \frac{1}{15} \left[S_i^\dagger (\delta_{ji} + i\epsilon_{jik} \sigma_k) S_j + 3\vec{S}^T \cdot \vec{S} \right] = \frac{1}{3} \vec{S}^T \cdot \vec{S} = \frac{1}{3} I_{4 \times 4}, \end{aligned} \quad (100)$$

where $i\epsilon_{jik} S_i^\dagger \sigma_k S_j = I_{4 \times 4}$, and $I_{4 \times 4}$ is the 4×4 unit matrix. Thus, we have

$$\Sigma_{nO}^{(3p)}(p) = -\frac{2}{15} \frac{y_{3p}^2 \mu_{nO}}{\mu_{nO}^4} \frac{\mu_{nO}}{2\pi} D'^{5/2} = \frac{2}{15} \frac{y_{3p}^2 \mu_{nO}}{\mu_{nO}^4} \frac{\mu_{nO}}{2\pi} (ip'^5). \quad (101)$$

- α - ^{13}C loops

The self-energy term from the α - ^{13}C loop for the $1/2^+$ state is obtained as [12]

$$\Sigma_{\alpha C}^{(1p)}(p) = \frac{y_{1p}^2}{3\mu_{\alpha C}^2} \left(\frac{\mu_{\alpha C}}{2\pi} 2\kappa H_1(p) \right), \quad (102)$$

where the function $H_1(p)$ is given in Eq. (14).

The self-energy term of α - ^{13}C loop for the $5/2^-$ state is obtained as

$$\Sigma_{\alpha C}^{(5m)}(p) = \frac{2y_{5m}^2}{15\mu_{\alpha C}^4} \left(\frac{\mu_{\alpha C}}{2\pi} 2\kappa H_2(p) \right), \quad (103)$$

where we used the relations,

$$R_a^\dagger L_b^\dagger L_x R_y \frac{1}{15} \left(\delta_{ax} \delta_{by} + \delta_{ay} \delta_{bx} - \frac{2}{3} \delta_{ab} \delta_{xy} \right) = \frac{2}{3} I_{6 \times 6}, \quad (104)$$

with

$$R_a^\dagger L_b^\dagger L_b R_a = R_a^\dagger L_b^\dagger L_a R_b = 5I_{6 \times 6}, \quad \vec{L} \cdot \vec{R} = 0, \quad (105)$$

and $I_{6 \times 6}$ is the 6×6 unit matrix.

The self-energy term of α - ^{13}C loop for the $3/2^+$ resonant state of ^{17}O is obtained as

$$\Sigma_{\alpha C}^{(3p)}(p) = \frac{y_{3p}^2}{3\mu_{\alpha C}^2} \left(\frac{\mu_{\alpha C}}{2\pi} 2\kappa H_1(p) \right). \quad (106)$$

C.4 Dressed propagators

The inverse of dressed propagators of the resonant states are obtained, as presented Feynman diagrams in Fig. 1, by including the self-energy terms. We obtain them in the center-of-mass frame as

$$D_S(p)^{-1} = \sum_{n=0}^N C_S^{(n)} E^n + \Sigma_{\alpha C}^{(S)}(p) + \Sigma_{nO}^{(S)}(p), \quad (107)$$

where S are labels for the resonant $1/2^+$, $5/2^-$, $3/2^+$ states of ^{17}O with $S = 1p, 5m, 3p$, and p is the magnitude of the relative momentum, $p = |\vec{p}|$, and $E = p_0 = p^2/(2\mu)$.

Thus, the inverse of the dressed propagators of the resonant states of ^{17}O in the center-of-mass frame are composed as

$$\begin{aligned} D_{1p}(p)^{-1} &= \sum_{n=0}^N C_{1p}^{(n)} p_0^n + \Sigma_{\alpha C}^{(1p)}(p) + \Sigma_{nO}^{(1p)}(p) \\ &= \sum_{n=0}^N C_{1p}^{(n)} E^n + \frac{y_{1p}^2}{3\mu^2} \left(\frac{\mu}{2\pi} 2\kappa H_1(p) \right) + y_{1p}^2 \frac{\mu'}{2\pi} (ip'), \\ D_{5m}(p)^{-1} &= \sum_{n=0}^N C_{5m}^{(n)} E^n + \Sigma_{\alpha C}^{(5m)}(p) + \Sigma_{nO}^{(5m)}(p) \end{aligned} \quad (108)$$

$$= \sum_{n=0}^N C_{5m}^{(n)} E^n + \frac{2y_{5m}^2}{15\mu^4} \left(\frac{\mu}{2\pi} 2\kappa H_2(p) \right) + \frac{2y_{5m}'^2}{45\mu'^6} \frac{\mu'}{2\pi} (ip'^7), \quad (109)$$

$$\begin{aligned} D_{3p}(p)^{-1} &= \sum_{n=0}^N C_{3p}^{(n)} p_0^n + \Sigma_{\alpha C}^{(3p)}(p) + \Sigma_{nO}^{(3p)}(p) \\ &= \sum_{n=0}^N C_{3p}^{(n)} E^n + \frac{y_{3p}^2}{3\mu^2} \left(\frac{\mu}{2\pi} 2\kappa H_1(p) \right) + \frac{2}{15} \frac{y_{3p}'^2}{\mu'^4} \frac{\mu'}{2\pi} (ip'^5), \end{aligned} \quad (110)$$

where E is the energy of the α - ^{13}C system in the center-of-mass frame, $p = \sqrt{2\mu E}$, $p' = \sqrt{2\mu'(E + Q)}$, and Q is the Q -value, $Q = 2.22$ MeV.